Design of homogeneous and heterogeneous human equivalent thorax phantom for tissue inhomogeneity dose correction using TLD and TPS measurements

S. Senthilkumar

Department of Radiotherapy, Madurai Medical College and Govt. Rajaji Hospital, Maduari-625 020, India

ABSTRACT

► *Original article*

* Corresponding author:
Dr. S. Senthilkumar,
Fax: *+91 4522532536*
E-mail:
     sasenthilgh@gmail.com

Background: The purpose of this study is to fabricate inexpensive in-house low cost homogeneous and heterogeneous human equivalent thorax phantom and assess the dose accuracy of the Treatment Planning Systems (TPS) calculated values for different lung treatment dosimetery. It is compared with Thermoluminescent Dosimeter (TLD) measurement. ***Materials and Methods***: Homogeneous and heterogeneous thorax human equivalent phantoms were fabricated using bee's wax (density=0.99 g/cm^3) as a tissue simulating material, with inserts of cork (density=0.2 g/cm^3) and Teflon (density=2 g/cm^3) as lung and spine simulating material respectively. Lithium fluoride (LiF) TLD capsules were irradiated for different thoracic tumor treatment techniques using the locally fabricated homogeneous and heterogeneous phantoms. The 3D TPS calculated values of homogeneous and heterogeneous phantoms were compared with TLD measured values. ***Results***: Experiments were carried out for different thoracic tumour treatment techniques for small and larger field sizes and also with and without wedge for Cobalt – 60 photon beams. Plato TPS were used to calculate the inhomogeneity for the homogeneous and heterogeneous phantoms. TLD and 3D TPS calculated values were found to have deviation of ± 5%. ***Conclusion***: Both the homogeneous and heterogeneous phantoms has proved to be a valuable tools in the development and implementation of external beam radiotherapy (EBRT) in the clinical thorax region and in the verification of absolute dose and dose distributions in the regions of clinical and dosimetric interest.

Keywords: *Homogeneous phantom, heterogeneous phantom, TLD, thoracic region tumour, TPS.*

INTRODUCTION

The accuracy of external beam radiotherapy has improved rapidly in recent years with the advancement of technology. New modalities like three-dimensional (3D) conformal radiotherapy, IMRT (intensity modulated radiotherapy) based on multi-leaf collimator (MLC) and Tomotherapy technology for cancer treatments have been adopted in radiotherapy centers. In many developing countries like India these facilities have not yet been widely used in many of the centres and the only equipment commonly available for external beam radiotherapy is a Co-60 machine [1]. The human body consists of a variety of tissues and cavities with different

physical and radiological properties. Most important among these are tissue and cavities that are radiologically different from water, including lungs, oral cavities, teeth, nasal passages, sinuses and bones. In the presence of such heterogeneities, it is essential that the absorbed dose delivered to all irradiated tissues is predicted accurately in order to maximize the therapeutic benefit of radiation therapy [2-5]. These heterogeneities can clearly disturb dose distribution during radiation therapy. Hence, it is incorrect to calculate dose distribution by assuming that the human body of a patient is homogeneous.

Accurate calculation necessitates an understanding of the heterogeneous nature of the human body and the path of incident photons through heterogeneities. Since it is essential to maximize the dose to the treatment volume while minimizing it to the normal surrounding tissue, the tumor outline must be accurately defined. For an optimum treatment of cancer, the radiation dose must be planned and delivered with a high degree of accuracy. The International Commission on Radiation Units and Measurements (ICRU) recommends that the dose to be delivered with an accuracy error of less than ± 5 % [6]. However, only an error of ± 3 % to ± 3.5 % in the overall process has been recommended [7, 8].

Dose distributions were generally calculated by assuming that the patient was composed entirely of water till the 1970s. This was mainly due to the lack of patient-specific anatomical information. With the advent of computerized tomography (CT) it is easy to derive electron density information *in–vivo*, which could be incorporated into the dose calculation process. This, in combination with tremendous advances in computer technology, resulted in much research with the aim of improving dose calculation procedures, which account for the complex physical process associated with the irradiation of the heterogeneous human body. All of this information can be processed for the improved delineation of diseased and normal tissues within the body. Yet, in spite of this sophisticated technology, many radiation therapy departments have only achieved limited use of imaging data in the dose calculation process. In fact, many cancer centers still do not use patient-specific tissue density corrections. This may be due in part to the cost and effort of implementing new imaging technologies, limited access to these technologies in individual radiation therapy institutions, and the variability in the implementation and capabilities of tissue heterogeneity corrections. These limitations complicate the standardization of dose delivery and contribute to uncertainties when comparing clinical outcomes.

Radiation oncologists have disregarded the effects of difference in density of the electron and physical density in the human body. Algorithms attempting to correct the density differences (Effective Path Length (EPL), TAR, and power law) were based on scaling beam data measured in a water phantom according to physical densities [9].

Treatment planning systems (TPS) provide a heterogeneity correction algorithm to convert dose calculation in a homogeneous water-like patient to the situation with heterogeneities. Although the influence of heterogeneities on the primary photon fluence is generally well predicted, the influence of heterogeneities on the dose delivered by scattered radiation is often approximated in a crude way. Most heterogeneity correction algorithms are semi-empirical and accurate only for a limited set of simplified geometries [10]. As a result, large dosimetric errors may occur in clinically relevant situations [11, 12].

Thermoluminescent Dosimeters (TLD) are used in radiotherapy to verify the radiation dose received by cancer patients. TLDs are being widely used for dosimetry in view of their availability in very small size as well as their ability to provide high spatial resolution with acceptable precision and accuracy, even at the sites of steep dose gradients in the vicinity of the sources [13-16]. The objective of this work is to study the heterogeneous dose distribution of lung cancer patients. TLD and 3D TPS data were compared in the in-house human tissue equivalent heterogeneous and homogeneous phantoms.

Int. J. Radiat. Res., Vol. 12 No. 2, April 2014

170

MATERIALS AND METHODS

Fabrication of heterogeneous phantom

A special thorax phantom was designated for this dosimetry study and is shown in figure 1 based on the ICRU report no.48 [17,18]. The body dimension of a normal Indian adult male was selected for the phantom fabrication. CT scan was done for this selected patient for the whole thorax region with 1.5 cm slice thickness. Each slice of the CT scan images was contoured. These contours consist of an outline of the body, both lungs and spine. The moulds were prepared with respect to the outline of the body contour of the CT scan images using wood. Bee's wax was used as a tissue simulating material. The cork and Teflon were used as lung and spine simulating material respectively. These materials were selected for its availability, low price and also for good machining property. The bee's wax has a density of 0.99 g/cm³. However, there are other appropriate phantom materials such as solid water, polystyrene and polyethylene [17]. 1.5 cm thickness of cork (density = 0.2 g/cm³) and Teflon (density = 2 g/cm³) were prepared with respect to the dimension of the each contour of the lung and spine respectively for all slices of the CT scan images. The prepared cork and Teflon materials were fixed in the appropriate place (lung and spine) of the mould with the help of CT external contours. Then the melted bees wax was poured inside the mould, which represent the tissue area of the mould. While pouring the melted wax into the mould, care was taken to avoid the formation of air bubbles and wax over the cork and Teflon.

Figure 1. Photograph of slices of heterogeneous thorax phantom, which was created for this study and used for dose measurement and calculation.

The phantom was removed from the mould after allowing the melted bee's wax to cool down. Similarly, the phantom was prepared for all the contours. Several holes were made in the bee's wax, cork and Teflon to keep the TLD for point dose measurement. These holes were completely filled with the same material with same size of cylinders. All the slices of the phantom were placed in position together, which resembles the exact human thorax heterogeneous phantom (figure 2).

Fabrication of homogeneous phantom

The homogeneous phantom (figure 3) was also prepared with the guidelines of the same CT scan images, which was used for the heterogeneous phantom. The preparation of homogeneous phantom was followed by the procedure adopted in heterogeneous phantom preparation. The homogeneous phantom was prepared without the incorporation of lung and spine areas. The holes were made in the homogeneous phantom for placing TLD capsules exactly at the same point as in the heterogeneous phantoms.

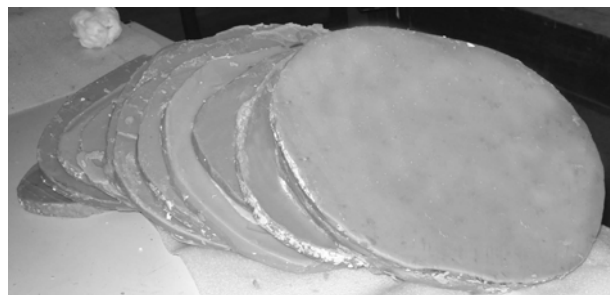**Figure 2.** Photograph of heterogeneous phantom in the treatment position with Co-60 machine.

Figure 3. Photograph of slices of homogeneous thorax phantom.

Thermoluminescent dosimeter

In this present study Lithium fluoride (LiF) TLD powder was used. This dosimeter system is well established as a known technique in measuring radiation dose during radiotherapy. It provides an accurate, reliable and low fading effect (less than 0.1% per day for LiF). In this study LiF TLD powder was placed in custom made reusable capsules. It was used as *in-vivo* dosimeter. The capsules were small cylinders with outer dimensions of 5 mm height and 5 mm diameter, with a 1 mm wall thickness. Each capsule was filled with appropriately 40 mg of powder, which yielded two readings. The capsules were constructed with high impact polystyrene, which contained very little air with the shape of a small sphere. The powder from capsule was used to evaluate the dose response, energy dependence, dose uniformity and fading. The accuracy of the thermoluminescent dosimetry system is ± 4% at the 90% confidence level.

Thermoluminescent recording was done by Nucleonic™ PC based TLD reader. The TLD reader was operated using a high voltage to its Photomultiplier (PM) tube to obtain the optimum signal to noise ratio. The time temperature profile using a heating rate of 10° C/s from a preset temperature of 50 to 300°C (maintained for 4.5 sec) was optimized and used for reading the TL glow curve for the integrated TL light output to cover the main TL glow peak occurring at 235°C at this heating rate[19]. TLD capsules were subjected to an annealing treatment of 400°C for 1 hour followed by 100° C for 2 hour and post irradiation annealing of 100° C for 10 min. prior to each read out.

3-D treatment planning systems

Nucletron 3D Plato version 3.3.1 was used for external beam radiotherapy planning to accurate the dose estimation. Heterogeneity correction implemented in this system was done by EPL method. It accepts the geometry of irradiation by a digitizer. The type of tissues and their density relative to water can be defined for each case.

The external contour, lungs and spine of thorax heterogeneous phantom were entered manually through digitizer into the TPS, in order to achieve an accurate reconstruction of the experimental geometry. The mass density of the phantom materials also was defined for TPS. Similarly all the slices of the heterogeneous thorax phantoms were digitized. A slice with large lung cavities was selected to be in the center of the fields. The measurement points were marked with uncertainty of less than 1 mm for dose calculations.

The relative dose of each point was calculated by considering one of the points in the field as a reference point, which is in the first point of the beam entrance inside the phantom. So, the effect of heterogeneity contribution to this point will be negligible. Similar method was adopted to enter the homogeneous thorax phantom external contour into the TPS.

Irradiation techniques

In the present work, five conventional techniques were used to study the effects of lungs and spine on the clinically used irradiation geometries in the thorax region. These irradiation techniques were used in the Theratron Phoenix Co-60 teletherapy machine, Canada. The heterogeneity phantom kept over the Co-60 machine treatment table as like the treatment position. The central ray of the photon beam was allowed to pass through the central slice of the heterogeneous phantom. TLD capsule were placed in the holes in the area of spine, media sternum, 12 in lungs, 1 in heart, 8 in ribs, entrance, exit and midpoint.

A dose of 100 cGy was prescribed. Both the heterogeneous and homogeneous phantoms were irradiated under the same treatment conditions. The following experimental set-ups were selected to resemble more closely to the clinical situation of thorax region radiotherapy.

Technique 1

An anterior mediastinal field is used in this technique, which is frequently used in the treatment of lung, mediasternum and esophageal cancer. Figure 4a and 4b represents the contour of the heterogeneous and homogeneous phantom for this technique.

Technique 2

Lateral and opposing lateral fields are used to

Int. J. Radiat. Res., Vol. 12 No. 2, April 2014

172

treat lung and mediastinal tumors. Contour of right and left lateral thorax field irradiation for heterogeneous phantom are shown in figure 5a and 5b respectively.

Technique 3

Anterior and posterior oblique fields are used for lung and esophageal tumors with different field sizes (figure 6a).

Technique 4

Posterior oblique fields with wedges are used for esophageal tumors with different field sizes (figure 6b).

Technique 5

An anterior large thorax field with a field size of 25 × 25 cm² is used. Figure 7a and 7b illustrates the heterogeneous and homogeneous phantom for large thorax field irradiation.
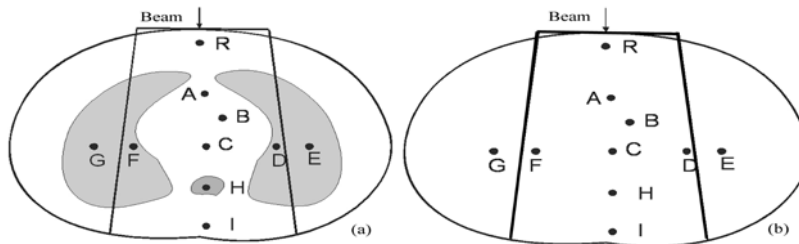

Figure 4. Schematic representation of anterior mediastinal field irradiation geometry for (a) heterogeneous and (b) homogeneous phantoms.
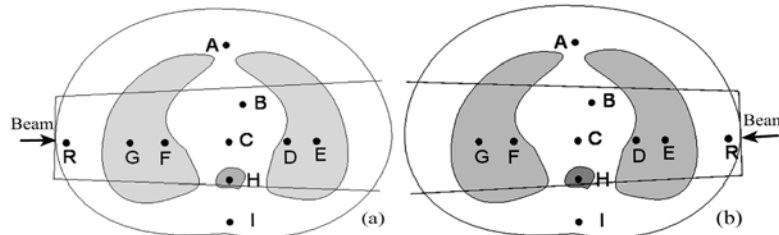

Figure 5. Schematic representation of (a) right and (b) left lateral thorax field irradiation geometry for heterogeneous phantoms.
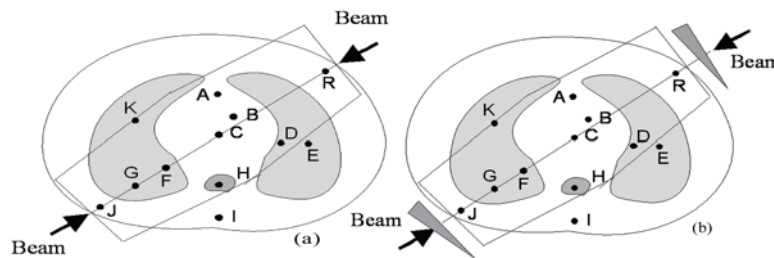

Figure 6. Schematic representation of anterior oblique field and posterior oblique field irradiation geometry for (a) without wedge and (b) with wedge for heterogeneous phantoms.
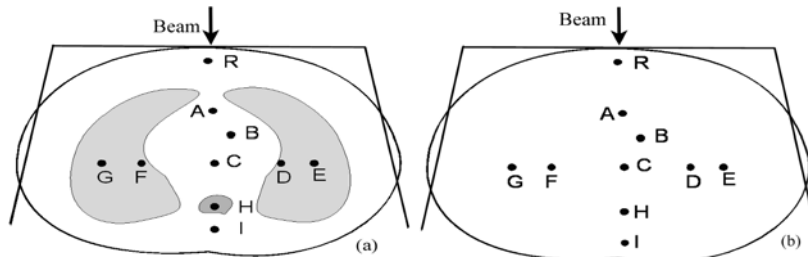

Figure 7. Schematic representation of anterior large thorax field irradiation geometry for (a) heterogeneous and (b) homogeneous phantoms.

RESULTS

The results were analyzed by comparing heterogeneous and homogeneous TPS calculated values with TLD measurements. This study has made use of different techniques for various field sizes of Co-60 machine and the TLD measurement and TPS output isodose chart calculation. But for convenience, only limited TLD and TPS readings for various techniques were presented in this paper. The results obtained by TLD and TPS values of homogeneous and heterogeneous medium for various techniques were analyzed.

Technique 1

The obtained TLD and TPS values for the irradiated heterogeneous and homogeneous in the anterior position phantom with anterior beam with field size of 10 ×10 cm^2 are compared in the table 1. It is noted from the table that the dose measured by the TLD and TPS (figure 8a) for heterogeneous phantom along the central axis shows less variation. There is a significant difference in absorbed dose in the lung region.

Technique 2

Here the phantom is exposed from right and left lateral (i.e) gantry angle 270° and 90° with the field size of 10 × 10 cm^2. From the table 2 and 3 it is observed that there is difference in dose absorption between homogeneous and heterogeneous mediums (figure 8b). It shows that the dose deposition is more or less same at reference point but there are more differences in lungs, heart, media sternum, spine, entrance and exit point. Figure 8c clearly shows that the dose difference between homogeneous and heterogeneous medium.

Technique 3

When both the homogeneous and heterogeneous medium were exposed for anterior and posterior opposed oblique field with gantry angle 240°, and 60° with field size of 10 ×10 cm^2, the dose at reference points are more or less same but there is more difference in lungs, heart, media sternum and in spine region, which is clearly shown in table 4, and the dose is compared at several point. The dose difference is clearly observed from figure 9.

Technique 4

Both the homogenous and heterogeneous medium was irradiated by the same procedure as in technique 3 but 30° wedge is used. Table 5 highlights the dose difference in important region such as lungs, heart, mediasternum and in spine. Air cavities in heterogeneous medium make this difference because of its less attenuation coefficient compared to tissues. Figure 10 shows the dose differences.
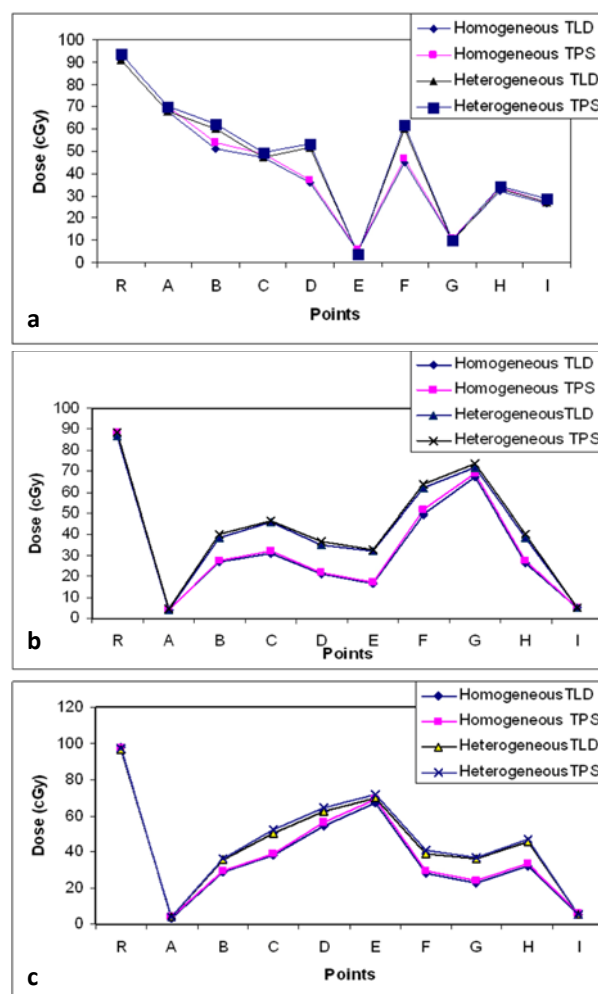

Figure 8. Figures shows the TPS and TLD values for homogenous and heterogeneous phantom for gantry angle 0°, 90°, 270° with field size of 10 X 10 cm^2.

Int. J. Radiat. Res., Vol. 12 No. 2, April 2014

174

Table 1. Comparison of TPS and TLD values for homogenous and heterogeneous phantom for gantry angle 0° with field size of 10 X 10 cm².

S. No.	Dose points in phantom	Homogeneous phantom (cGy)		Heterogeneous phantom (cGy)		Deviation for homogenous Phantom (%)	Deviation for heterogeneous Phantom (%)
		TLD	TPS	TLD	TPS		
1	R	91.1	93.6	91.2	93.6	2.74	2.63
2	A	68.2	70.4	67.9	70.4	3.23	3.68
3	B	51.4	53.7	60.2	62.3	4.47	3.49
4	C	47.2	48.7	47	49.3	3.18	4.89
5	D	35.7	37.3	51.8	53.2	4.48	2.70
6	E	5.3	5.5	3.98	4.1	3.77	3.02
7	F	44.9	46.6	60.1	61.9	3.79	3.00
8	G	9.98	10.4	9.45	9.9	4.21	4.76
9	H	32.1	33.7	33.4	34.4	4.98	2.99
10	I	26.2	27	27.2	28.4	3.05	4.41

Table 2. Comparison of TPS and TLD values for homogenous and heterogeneous phantom for gantry angle 90°.

S. No.	Dose points in phantom	Homogeneous phantom (cGy)		Heterogeneous phantom (cGy)		Deviation for homogenous Phantom (%)	Deviation for heterogeneous Phantom (%)
		TLD	TPS	TLD	TPS		
1	R	98.1	97.4	96.8	97.3	-0.71	0.52
2	A	3.65	3.9	4.1	4.3	6.85	4.88
3	B	28.9	29.7	35.4	36.5	2.77	3.11
4	C	38.1	38.9	50.4	52.4	2.10	3.97
5	D	54.2	56.1	62.1	64.5	3.51	3.86
6	E	67.2	69.2	69.5	71.8	2.98	3.31
7	F	27.9	29.2	38.9	40.8	4.66	4.88
8	G	23.1	23.8	35.9	37	3.03	3.06
9	H	32.4	33.8	45.7	47.1	4.32	3.06
10	I	5.48	5.7	5.4	5.5	4.01	1.85

Table 3. Comparison of TPS and TLD values for homogenous and heterogeneous phantom for gantry angle 270° with field size of 10 X 10 cm².

S. No.	Dose points in phantom	Homogeneous phantom (cGy)		Heterogeneous phantom (cGy)		Deviation for homogenous Phantom (%)	Deviation for heterogeneous Phantom (%)
		TLD	TPS	TLD	TPS		
1	R	86.50	88.70	86.90	88.70	2.54	2.07
2	A	3.90	3.80	4.30	4.50	-2.56	4.65
3	B	27.10	27.60	38.50	40.00	1.85	3.90
4	C	30.80	31.90	45.80	46.50	3.57	1.53
5	D	21.20	21.80	35.20	36.70	2.83	4.26
6	E	16.80	17.30	32.00	33.00	2.98	3.13
7	F	49.38	51.80	61.90	63.80	4.90	3.07
8	G	67.10	69.10	71.80	73.60	2.98	2.51
9	H	26.40	27.70	38.50	40.00	4.92	3.90
10	I	5.20	5.40	5.40	5.20	3.85	-3.70

Table 4. Comparison of TPS and TLD values for homogenous and heterogeneous phantom for anterior and posterior oblique fields.

S. No.	Dose points in phantom	Homogeneous phantom (cGy)		Heterogeneous phantom (cGy)		Deviation for homogenous Phantom (%)	Deviation for heterogeneous Phantom (%)
		TLD	TPS	TLD	TPS		
1	R	96.80	98.20	96.20	98.20	1.45	2.08
2	A	6.80	7.00	5.15	5.00	2.94	-2.91
3	B	64.80	66.20	74.20	76.80	2.16	3.50
4	C	64.20	66.00	75.90	79.40	2.80	4.61
5	D	69.50	71.30	81.10	83.90	2.59	3.45
6	E	73.10	75.20	76.20	79.70	2.87	4.59
7	F	67.20	69.30	78.60	80.50	3.12	2.42
8	G	73.70	75.80	81.40	83.30	2.85	2.33
9	H	62.40	64.80	70.70	73.70	3.85	4.24
10	I	16.10	16.80	16.10	16.70	4.35	3.73

Table 5. Comparison of TPS and TLD values for homogenous and heterogeneous phantom for anterior and posterior oblique fields with wedge.

| S. No.	Dose points in phantom	Homogeneous phantom (cGy)		Heterogeneous phantom (cGy)		Deviation for homogenous Phantom (%)	Deviation for heterogeneous Phantom (%)
		TLD	TPS	TLD	TPS		
1	R	87.40	88.50	86.80	88.50	1.26	1.96
2	A	6.20	6.40	4.50	4.70	3.23	4.44
3	B	44.20	45.10	51.20	53.40	2.04	4.30
4	C	54.20	56.10	67.20	68.80	3.51	2.38
5	D	58.10	60.60	72.90	74.50	4.30	2.19
6	E	68.20	67.10	75.10	77.50	-1.61	3.20
7	F	56.20	58.90	67.80	69.70	4.80	2.80
8	G	62.50	64.80	71.60	72.60	3.68	1.40
9	H	63.90	64.80	71.70	73.70	1.41	2.79
10	I	14.90	15.40	15.50	16.00	3.36	3.23
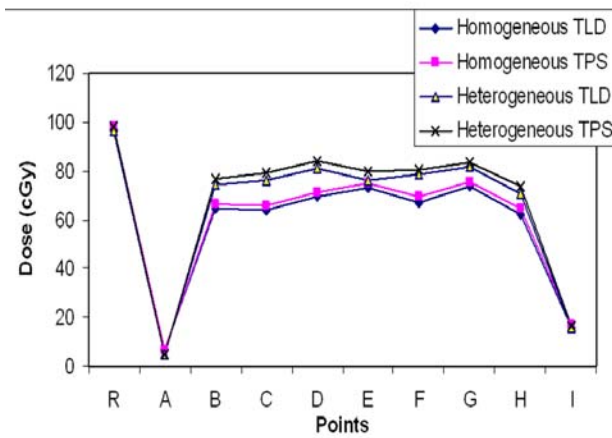
Figure 9. TPS and TLD values for homogenous and heterogeneous phantom for anterior and posterior oblique fields.
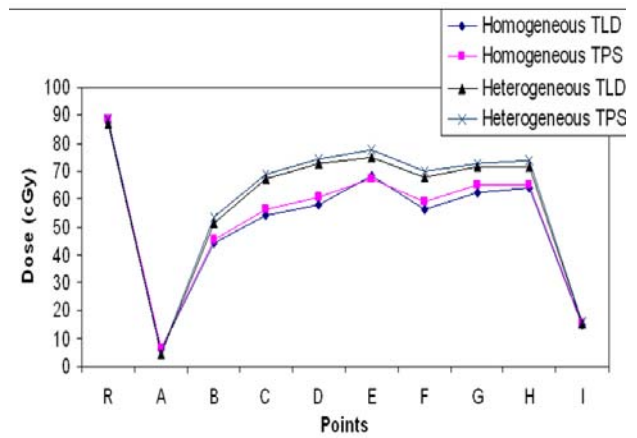

Figure 10. TPS and TLD values for homogenous and heterogeneous phantom for anterior and posterior oblique fields with wedge.

Int. J. Radiat. Res., Vol. 12 No. 2, April 2014

176

Technique 5

When the thorax is irradiated in anterior position with wider field size of 25 × 25 cm², the dose difference is more in lungs between the homogeneous and heterogeneous medium. Table 6 shows the dose difference in important region. The dose difference in lung is clearly shown in figure 11.

TLD Vs TPS

To verify the TPS reading, LiF TLD's were used. TPS values were compared with TLD value for both homogeneous and heterogeneous medium for different techniques. The percentage deviations of TLD and TPS for both mediums were calculated using the formula: $E=[(C-M)/M] \times 100$, where E is percentage of error between homogeneous and heterogeneous phantom, C is calculated values of TPS and M is the measurement of TLD for both phantoms.
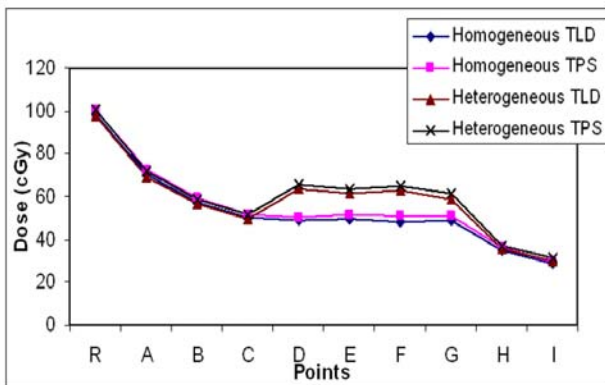

Figure 11. TPS and TLD values for homogenous and heterogeneous phantom for gantry angle 0° with Full open.

Percentage deviation between TPS and TLD readings lies between in ±5% for all techniques.

The tissue heterogeneity contributes to the dose uncertainty in the external beam radiotherapy. The results of our experiment indicated that the perturbation occurred in dose distribution due to the air inhomogeneity. If one neglects the air tissue inhomogeneity near the treatment volume the treatment planning in Co-60 can lead to inaccurate dose planning. However, any heterogeneity correction is better than none at all [20].

DISCUSSION

In the case of first technique the difference in the dose estimation in the lung region is due to the fact that the photon attenuation is less in lung medium owing to the presence of air cavities and more attenuation in the homogeneous medium. For the second technique the dose at reference points is same because of same tissue attenuation in both homogeneous and heterogeneous mediums. The variation in the dose measurement points for heterogeneous objects in the thoracic region is due to less attenuation in air cavities of lungs in heterogeneous medium which makes the attenuation in air which makes the photon beam to deposit more doses in heart, mediasternum, spine and in exit point region compared to homogeneous medium which have more attenuation coefficient. The scatter contribution

Table 6. Comparison of TPS and TLD values for homogenous and heterogeneous phantom for anterior field with full open.

S. No.	Dose points in phantom	Homogeneous phantom (cGy)		Heterogeneous phantom (cGy)		Deviation for homogenous Phantom (%)	Deviation for heterogeneous Phantom (%)
		TLD	TPS	TLD	TPS		
1	R	98.50	100.30	97.50	100.30	1.83	2.87
2	A	70.20	72.90	69.20	71.90	3.85	3.90
3	B	57.30	59.00	56.40	58.90	2.97	4.43
4	C	50.10	51.90	49.80	51.80	3.59	4.02
5	D	48.90	50.50	63.50	65.60	3.27	3.31
6	E	49.60	51.40	61.40	63.70	3.63	3.75
7	F	48.30	51.10	62.90	64.90	5.80	3.18
8	G	48.70	50.80	58.90	61.30	4.31	4.07
9	H	35.10	36.60	35.80	37.00	4.27	3.35
10	I	28.50	29.60	29.80	31.10	3.86	4.36

in the thoracic region is less in homogeneous medium compared to heterogeneous medium. For the oblique fields, the dose difference in the thoracic regions is due to less attenuation coefficient of air cavities in heterogeneous medium. In the case of oblique fields with wedges the dose differences in the thoracic region is also due to air cavities in heterogeneous medium which has got less attenuation coefficient.

CONCLUSION

Homogeneous and heterogeneous human tissue equivalent thorax phantom were successfully fabricated, using bee's wax, cork and Teflon material. Both the TLD and TPS values were compared for homogeneous and heterogeneous phantoms. It can be concluded that the dose calculation by EPL based 3D TPS for thorax cancer radiotherapy treatments have acceptable for dose points and unit density materials. Hence, this study reveals that the thorax region is the main heterogeneous region. Whenever planning to deliver radiotherapy to cancer patient under heterogeneous conditions, homogeneity correction factor must be calculated to deliver accurate dose to the tumor volume. Heterogeneity corrections are particularly important during external beam radiotherapy, particularly in lung cancer treatment. The benefits of accounting for tissue inhomogeneity vastly outweigh the minor difficulties with its implementation with result in more accurate calculation of dose distribution and hopefully in better outcomes of the patient.

REFERENCES

1. Geroge X Ding, Dennis M Duggan, Bo Lu (2007) Impact of inhomogeneity corrections on dose coverage in the treatment of lung cancer using stereotactic body radiation therapy. *Med Phys,* **34(7):** 2985-2994.
2. Senthilkumar S and Ramakrishnan V (2011) Fabrication of low cost in-house slab homogeneous and heterogeneous phantoms for lung radiation treatment. *Iran J Radiat Res,* **9(2):** 109-119.
3. Don Robinson (2008) Inhomogeneity correction and the analytic anisotropic algorithm. *J Appl Clin Med Phys,* **9(2):** 112—122.
4. Tissue inhomogeneity corrections for megavoltage photon beams AAPM report no. 85, (2004) Madison, USA: AAPM.
5. Anuj Kumar, Sunil Dutt Sharma, Arya AK, Surabhi Gupta, Deepak Shrotriya (2011) Effect of low-density heterogeneities in telecobalt therapy and validation of dose calculation algorithm of a treatment planning system. *J Med Phys,* **36(4):** 198–204.
6. Svenesson GK (1984) Quality assurance in radiation therapy: physical effort. *Int J Radiat Oncol Biol Phys,* **10(suppl 1):** 23-29.
7. Brahme A, Chavaudra J, Landberg T (1988) Accuracy requirements and quality assurance of external beam therapy with photons and electrons. *Acta Oncol,* **(Suppl 1):** 1-76.
8. Venselaar J, Welleweerd H, Mijnheer B (2001) Tolerances for the accuracy of photon beam dose calculations of treatment planning systems. *Radiother Oncol,* **60:** 191-201.
9. Andrew O Jones, Indra J Das, Frederick L Jones (2003) A Monte Carlo study of IMRT beamlets in inhomogeneous media. *Med Phys,* **30(3):** 296-300.
10. ICRU Report 42 (1987) Use of computers in external beam radiotherapy procedures with high energy photons and electrons. Washington, DC: International Commission on Radiation Units and Measurement.
11. Ekstrand KE and Barnes WH (1990) Pitfalls in the use of high energy X-rays to treat tumors in the lung. *Int J Radiat Oncol Biol Phys,* **18:** 249-252.
12. El-Khatib EE, Evans M, Pla M (1989) Evaluation of lung dose correction methods for photon irradiation of thorax phantoms. *Int J Radiat Oncol Biol Phys,* **17:** 871-878.
13. Anctil J, Clark BG, Arsenault CJ (1998) Experimental determination of dosimetry functions of Ir-192 sources. *Med Phys,* **25:** 2279-2287.
14. Karaiskos P (1998) Monte Carlo and TLD dosimetry of an ^{192}Ir high dose rate brachytherapy source. *Med Phys,* **25:** 1975-1984.
15. Kirov AS, Williamson JF, Meigooni AS (1995) TLD, diode and Monte Carlo dosimetry of an ^{192}Ir for high dose rate brachytherapy. *Phys Med Biol,* **40:** 2015-2036.
16. David Followill, DeeAnn Radford Evans (2007) Design, development, and implementation of the Radiological Physics Center's pelvis and thorax anthropomorphic quality assurance phantoms. *Med Phys,* **34(6):** 2070-2076.
17. Nath R (1995) Dosimetry of interstitial brachytherapy source: Recommendations of AAPM radiation therapy committee task group no. 43. *Med Phys,* **22:** 209-234.
18. ICRU Report 48 (1992) Phantoms and computational models in therapy, diagnosis and protection. Maryland, USA. International Commission on Radiation Units and Measurement, **15**.
19. Pradhan AS (1995) Influence of heating rate on the response of TLDs. *Radiat Prot Dosim,* **58:** 205-209.
20. Photon treatment planning collaborative working group (1991) Role of inhomogeneity corrections in three–dimensional photon treatment planning. *Int J Radiat Oncol Biol Phys,* **21:** 59-69.

Int. J. Radiat. Res., Vol. 12 No. 2, April 2014

178